Smart Structures and Systems, *Vol. 13, No. 5 (2014) 869-890*
DOI: http://dx.doi.org/10.12989/sss.2014.13.5.869

A structural damage detection approach using train-bridge interaction analysis and soft computing methods

Xingwen He*[1], Mitsuo Kawatani[2], Toshiro Hayashikawa[1], Chul-Woo Kim[2], F. Necati Catbas[3] and Hitoshi Furuta[4]

[1]*Faculty of Engineering, Hokkaido University, Sapporo 060-8628, Japan*
[2]*Graduate School of Engineering, Kobe University, Kobe 657-8501, Japan*
[3]*Department of Civil, Environ. and Constr. Eng., University of Central Florida, Orlando, FL 32816-2450, USA*
[4]*Faculty of Informatics, Kansai University, Osaka 569-1095, Japan*

(Received December 1, 2012, Revised August 28, 2013, Accepted August 30, 2013)

Abstract. In this study, a damage detection approach using train-induced vibration response of the bridge is proposed, utilizing only direct structural analysis by means of introducing soft computing methods. In this approach, the possible damage patterns of the bridge are assumed according to theoretical and empirical considerations at first. Then, the running train-induced dynamic response of the bridge under a certain damage pattern is calculated employing a developed train-bridge interaction analysis program. When the calculated result is most identical to the recorded response, this damage pattern will be the solution. However, owing to the huge number of possible damage patterns, it is extremely time-consuming to calculate the bridge responses of all the cases and thus difficult to identify the exact solution quickly. Therefore, the soft computing methods are introduced to quickly solve the problem in this approach. The basic concept and process of the proposed approach are presented in this paper, and its feasibility is numerically investigated using two different train models and a simple girder bridge model.

Keywords: damage detection; bridge diagnosis; train-bridge interaction; soft computing; health monitoring

1. Introduction

In the high-speed railway system nowadays, which is constructed nearly 50 years ago and Shinkansen in Japan, efficient health monitoring and diagnosis of viaduct structures become especially important in maintenance work, because the viaducts account for a large proportion of main line structures. Currently, the overall health condition of the Shinkansen viaducts is mainly examined by visual inspections, which demand a large number of technicians and also a considerable cost because of the huge number of structures. Owing to the decreasing birthrate as well as the aging society in Japan, it is important to develop more effective and economical health monitoring and diagnosis approaches for civil infrastructure.

It is already reported (Doebling *et al*. 1998, Alvandi and Cremona 2006, Siringoringo and Fujino 2006, Ni *et al*. 2008) that it is possible to conveniently use the dynamic characteristics of

∗Corresponding author, Assistant Professor, E-mail: xingwen_he@eng.hokudai.ac.jp

http://www.techno-press.org/?journal=sss&subpage=8 ISSN: 1738-1584 (Print), 1738-1991 (Online)

the bridge to identify the structural conditions. However, using what kind of dynamic response of the bridge for damage detection is an essential issue in vibration-based health monitoring problems. For long-span bridges, micro-tremors of structures due to wind loads, ground vibrations, etc can be used for health monitoring (Siringoringo and Fujino 2006). However, bridges like Shinkansen viaducts, most of which are short-span RC and steel structures, are usually insensitive to such micro-tremors. In fact, impact tests have been adopted to investigate the integrity of bridge structures on Shinkansen lines since 1991. However, the impact tests not only demand enormous manpower and cost, but also have the deficiency that it cannot be carried out during operational hours. If the dynamic bridge response induced by the running trains can be effectively used for the health monitoring and diagnosis process, it will be an economical and convenient way because the traffic-induced vibrations of Shinkansen viaducts have been continually recorded by not only the railway companies but also the local municipalities. However, cautious considerations are required to use the train-induced bridge vibration for damage identification because it is a kind of non-stationary process (Kim *et al*. 2005).

Some studies on bridge health monitoring and damage identification using traffic-induced vibration data have been initiated recently, in which inverse analyses are commonly required to carry out the identification (Yoshida *et al*. 2006, Kawatani *et al*. 2012, Kim and Kawatani 2008, Zhan *et al*. 2011, Kim and Isemoto *et al*. 2012, Kim and Kawatani *et al*. 2012). However, in some cases there are some difficulties such as the ill-posed problems for the inverse analysis to be applied to complicated structures (Yoshida *et al*. 2008). The numerical errors caused by the inverse analysis may grow significantly with increasing structural members, thus bringing difficulties in practical applications. To avoid difficulties faced by inverse analysis, a damage detection approach using only direct structural analysis of the train-induced bridge vibration is thus proposed in this research, which is realized by introducing soft computing methods.

In this approach, different from identifying the structural damages from the bridge vibration response using inverse analyses, the possible damage patterns of the bridge are assumed according to theoretical and empirical considerations at first. Then, the train-induced dynamic response of the bridge under a certain damage pattern is calculated employing a train-bridge interaction analysis program developed by the authors. When the calculated result is most identical to the recorded response, this damage pattern will be the solution. However, owing to the huge number of possible damage patterns, it is extremely time-consuming to calculate the bridge responses of all the cases and thus difficult to identify the exact solution quickly. Therefore, soft computing methods including Genetic Algorithm (GA) and Neural Network (NN) are introduced to quickly solve the problem in this approach. The basic concept and process of the proposed approach is presented in this paper, in which the application of NN is only introduced theoretically but not used in the identification process due to the simplicity of the bridge structure. Then, the feasibility of the proposed identification approach is numerically investigated using a simple girder bridge model and two-degree-of-freedom (2-DOF) as well as three-dimensional (3D) train models.

2. Concepts of the proposed approach

In recent years, the applications of soft computing methods such as GA (Perry *et al*. 2006, Koh and Perry 2009) and NN (Yun and Bahng 2000) in engineering fields including structural identification problems are indicating remarkable progress. In this research, a bridge damage detection approach is proposed employing only direct analyses of train-induced bridge vibration by means of introducing soft computing methods to avoid the numerical problems encountered in the inverse analysis. A bridge with a complicated structure theoretically suffers a myriad of damage patterns. However, in actual railway viaducts the possible damage patterns of the structure are comprehended by the bridge engineers based on theoretical and empirical facts. Therefore in this approach, the possible/detectable damage patterns of the bridge members are assumed in advance and used as the input information. Then, the train-induced dynamic response of the bridge under a certain damage pattern is calculated by a computer program. In the possible/detectable damage patterns, the one identical or nearest to the actual damage condition will give the most similar dynamic responses to the recorded ones, through which the exact solution can be identified. To make this approach applicable to actual structures with enormous possible damage patterns, the soft computing methods of NN and GA are proposed to be applied as follows.

2.1 Application of NN

In the proposed approach, the train-induced dynamic response of the bridge used to compare with measured ones will be simulated by a train-bridge interaction analysis computer program developed by the authors. However, for a large-scale structure, even one time of such an analysis will demand considerable computational cost, which will lead to difficulties in the actual identification process that needs a great number of interaction analyses. Therefore in this research, the NN techniques (Kartam *et al*. 1997) are planned to be used to simulate the train-induced bridge response, which, once established, can shorten the computational time of the identification process to an acceptable degree in actual applications. In this paper, for the preliminary development stage, to simplify the problem the establishment of the NN tool is ignored because of usage of simple structural model that only demands small computational capacities.

2.2 Application of GA

The calculated train-induced bridge responses under certain damage patterns are then used for the damage identification. However, even if only the possible damage patterns based on engineering facts are assumed, the number can still be considerable large and it is difficult to quickly find the exact solution. This is a typical combinatorial optimization problem and can be solved by some metaheuristic search algorithms. In this research, the GA technique (Goldber 1989) is adopted to quickly find the exact damage pattern. GA was formally introduced in the United States in the 1970s by John Holland at University of Michigan. GA works very well on mixed (continuous and discrete), combinatorial problems. They are less susceptible to getting stuck at local optima than gradient search methods. In the GA program, the damage patterns are set as the population and the difference between the calculated results and the recorded ones is defined as the objective function. It is obvious that the proper definition of the objective function can be a determinative factor for the identification results in actual applications.

3. Train-bridge interaction analysis procedure

In this paper, both real 3D and simplified train models together with a simple girder bridge model are used to examine the feasibility of the proposed approach. Considering their dynamic interaction, the train-induced bridge response is simulated with a developed computer program based on the formulation described in this chapter. Cars of the realistic train are idealized as 3D sprung-mass vibration systems, assuming that the car-body and the bogies are rigid bodies and that they are connected three-dimensionally by scalar spring and damper elements. The bridge structures are modeled as 3D beam elements and then formulated by FEM. Modal analysis technique is applied to the simultaneous differential equations of the structure. The Newmark's β step-by-step numerical integration method (Newmark 1959) is applied to solve the dynamic differential equations. The differential equations of train-bridge interaction system are derived as in the following sections.

3.1 Formulation of the train motion

Fig. 1 shows a train car modeled as 3D sprung-mass system. The variables employed in the car model are shown in Table 1. The notations of the train properties are indicated in Table 2. The definition of dimensions of the car is shown in Table 3. The differential equations of the train motion can be obtained based on D'Alembert's Principle as follows.

y_{j1}: Lateral translation of the car-body

$$m_1 \ddot{y}_{j1} - \sum_{l=1}^{2} \sum_{m=1}^{2} (-1)^m v_{jylm}(t) = 0 \tag{1}$$

z_{j1}: Bouncing of the car-body

$$m_1 \ddot{z}_{j1} + \sum_{l=1}^{2} \sum_{m=1}^{2} v_{jzlm}(t) = 0 \tag{2}$$

θ_{jx1}: Rolling of the car-body

$$I_{x1} \ddot{\theta}_{jx1} - \sum_{l=1}^{2} \sum_{m=1}^{2} (-1)^m \lambda_{y3} v_{jzlm}(t) - \sum_{l=1}^{2} \sum_{m=1}^{2} (-1)^m \lambda_{z1} v_{jylm}(t) = 0 \tag{3}$$

θ_{jy1}: Pitching of the car-body

$$I_{y1} \ddot{\theta}_{jy1} + \sum_{l=1}^{2} \sum_{m=1}^{2} (-1)^l \lambda_{x1} v_{jzlm}(t) = 0 \tag{4}$$

θ_{jz1}: Yawing of the car-body

$$I_{z1} \ddot{\theta}_{jz1} + \sum_{l=1}^{2} \sum_{m=1}^{2} (-1)^{l+m} \lambda_{x1} v_{jylm}(t) + \sum_{l=1}^{2} \sum_{m=1}^{2} (-1)^m \lambda_{y4} v_{jxlm}(t) = 0 \tag{5}$$

where

$$v_{jxlm}(t) = k_1 \left\{ (-1)^m \lambda_{y4} (\theta_{jz1} - \theta_{jz2l}) \right\} \tag{6}$$

$$\begin{aligned} v_{jylm}(t) = k_2 \left\{ -(-1)^m y_{j1} - (-1)^m \lambda_{z1} \theta_{jx1} + (-1)^{l+m} \lambda_{x1} \theta_{jz1} + (-1)^m y_{j2l} - (-1)^m \lambda_{z2} \theta_{jx2l} \right\} \\ + c_2 \left\{ -(-1)^m \dot{y}_{j1} - (-1)^m \lambda_{z1} \dot{\theta}_{jx1} + (-1)^{l+m} \lambda_{x1} \dot{\theta}_{jz1} + (-1)^m \dot{y}_{j2l} - (-1)^m \lambda_{z2} \dot{\theta}_{jx2l} \right\} \end{aligned} \tag{7}$$

$$
\begin{aligned}
v_{jzlm}(t) = {} & k_3\left\{z_{j1} + (-1)^l \lambda_{x1}\theta_{jy1} - (-1)^m \lambda_{y3}\theta_{jx1} - z_{j2l} + (-1)^m \lambda_{y3}\theta_{jx2l}\right\} \\
& + c_3\left\{\dot{z}_{j1} + (-1)^l \lambda_{x1}\dot{\theta}_{jy1} - (-1)^m \lambda_{y3}\dot{\theta}_{jx1} - \dot{z}_{j2l} + (-1)^m \lambda_{y3}\dot{\theta}_{jx2l}\right\}
\end{aligned}
\tag{8}
$$

where, the subscripts relative to the motion of the car-body are described as follows: l=1, 2 respectively indicate the front and rear bogies; m=1, 2 respectively indicate the left and right sides of the train. j is the sequence number of the car. $v_{jxlm}(t)$, $v_{jylm}(t)$ and $v_{jzlm}(t)$ denote the forces caused by the extension of the upper springs in relative directions, respectively.

y_{j2l}: Sway of the bogie

$$
m_2\ddot{y}_{j2l} + \sum_{m=1}^{2}(-1)^m v_{jylm}(t) - \sum_{k=1}^{2}\sum_{m=1}^{2}(-1)^m v_{jylkm}(t) = 0 \tag{9}
$$

z_{j2l} :Parallel hop of the bogie

$$
m_2\ddot{z}_{j2l} - \sum_{m=1}^{2} v_{jzlm}(t) + \sum_{k=1}^{2}\sum_{m=1}^{2} v_{jzlkm}(t) = 0 \tag{10}
$$

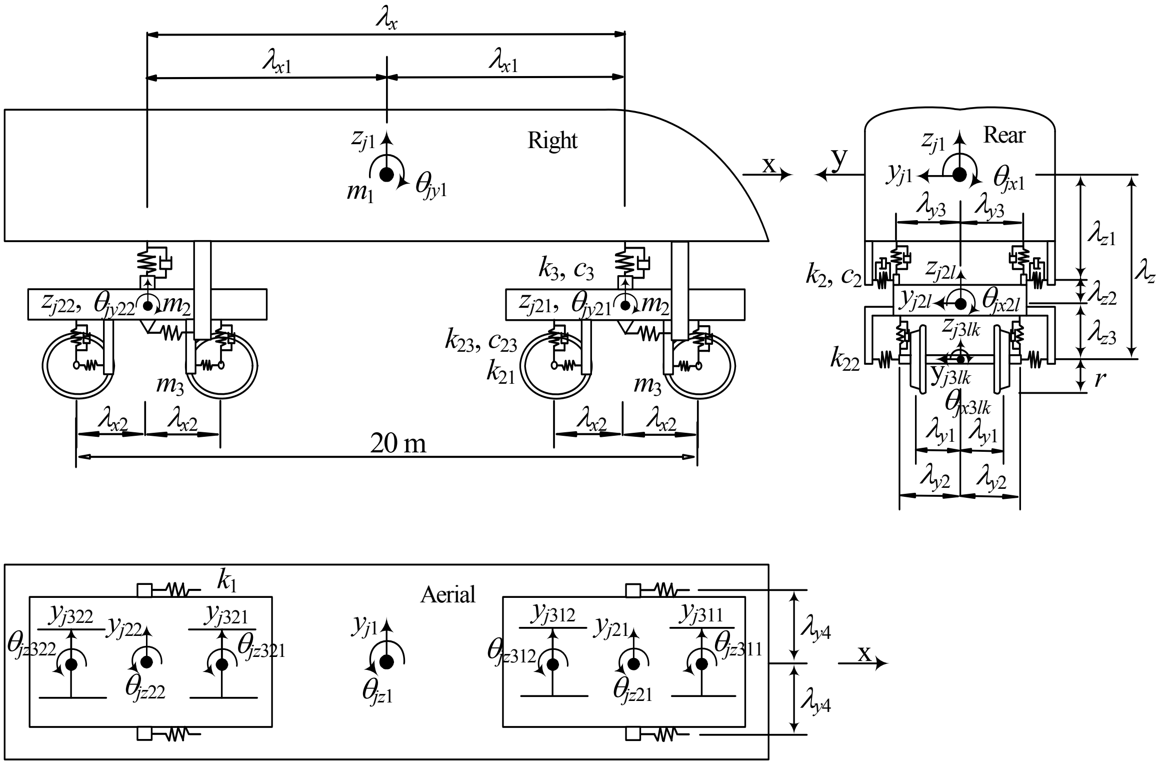

Fig. 1 Sprung-mass dynamic train car 3D model

Table 1 Variables employed in train model

Definition (j^{th} car)	Notation
Lateral translation of car body	y_{j1}
Sway of front bogie	y_{j21}
Sway of rear bogie	y_{j22}
Bouncing of car body	z_{j1}
Parallel hop of front bogie	z_{j21}
Parallel hop of rear bogie	z_{j22}
Rolling of car body	θ_{jx1}
Axle tramp of front bogie	θ_{jx21}
Axle tramp of rear bogie	θ_{jx22}
Pitching of car body	θ_{jy1}
Windup of front bogie	θ_{jy21}
Windup of rear bogie	θ_{jy22}
Yawing of car body	θ_{jz1}
Yawing of front bogie	θ_{jz21}
Yawing of rear bogie	θ_{jz22}

Table 2 Properties of the train model

Definition	Notation	Value
Weight of car body	w_1	321.6 kN
Weight of bogie	w_2	25.9 kN
Weight of wheel	w_3	8.8 kN
Mass moment of inertia of car body	I_{x1}	49.2 kN·s^2·m
	I_{y1}	2512.6 kN·s^2·m
	I_{z1}	2512.6 kN·s^2·m
Mass moment of inertia of bogie	I_{x2}	2.9 kN·s^2·m
	I_{y2}	4.1 kN·s^2·m
	I_{z2}	4.1 kN·s^2·m
Spring constant	k_1	5000 kN/m
	k_2	176.4 kN/m
	k_3	443 kN/m
	k_{21}	17500 kN/m
	k_{22}	4704 kN/m
	k_{23}	1210 kN/m
Damping coefficient	c_2	39.2 kN·s/m
	c_3	21.6 kN·s/m
	c_{23}	19.6 kN·s /m

Table 3 Definition of dimensions of the train model

1/2 length of car body in x-direction	c	12.50 m
Distance of centers of bogies in x-direction	x	17.50 m
1/2 distance of centers of bogies in x-direction	$x1$	8.75 m
1/2 distance of axes in x-direction	$x2$	1.25 m
1/2 width of track gauge	$y1$	0.70 m
1/2 distance of vertical lower springs in y-direction	$y2$	1.00 m
1/2 distance of vertical upper springs in y-direction	$y3$	1.23 m
1/2 distance of longitudinal upper springs in y-direction	$y4$	1.42 m
Distance from centroid of body to axis in z-direction	z	0.97 m
Distance from centroid of body to lateral upper spring in z-direction	$z1$	0.50 m
Distance from centroid of bogie to lateral upper spring in z-direction	$z2$	0.37 m
Distance from centroid of bogie to lateral lower spring in z-direction	$z3$	0.10 m
Radius of wheel	r	0.43 m

θ_{jx2l} :Axle tramp of the bogie

$$\begin{aligned} I_{x2}\ddot{\theta}_{jx2l} - \sum_{m=1}^{2}(-1)^m \lambda_{z2} v_{jylm}(t) + \sum_{m=1}^{2}(-1)^m \lambda_{y3} v_{jzlm}(t) \\ - \sum_{k=1}^{2}\sum_{m=1}^{2}(-1)^m \lambda_{z3} v_{jylkm}(t) - \sum_{k=1}^{2}\sum_{m=1}^{2}(-1)^m \lambda_{y2} v_{jzlkm}(t) = 0 \end{aligned} \tag{11}$$

θ_{jy2l} :Windup motion of the bogie

$$I_{y2}\ddot{\theta}_{jy2l} + \sum_{k=1}^{2}\sum_{m=1}^{2}(-1)^k \lambda_{x2} v_{jzlkm}(t) = 0 \tag{12}$$

θ_{jz2l} :Yawing of the bogie

$$I_{z2}\ddot{\theta}_{jz2l} - \sum_{m=1}^{2}(-1)^m \lambda_{y4} v_{jxlm}(t) + \sum_{k=1}^{2}\sum_{m=1}^{2}(-1)^{k+m} \lambda_{y2} v_{jxlkm}(t) + \sum_{k=1}^{2}\sum_{m=1}^{2}(-1)^{k+m} \lambda_{x2} v_{jylkm}(t) = 0 \tag{13}$$

where

$$v_{jxlkm}(t) = k_{21}\left\{(-1)^{k+m} \lambda_{y2}(\theta_{jz2l} - \theta_{jz3lk})\right\} \tag{14}$$

$$v_{jylkm}(t) = k_{22}\left\{-(-1)^m y_{j2l} - (-1)^m \lambda_{z3}\theta_{jx2l} + (-1)^{k+m} \lambda_{x2}\theta_{jz2l} + (-1)^m y_{j3lk}\right\} \tag{15}$$

$$\begin{aligned} v_{jzlkm}(t) = k_{23}\left\{z_{j2l} - (-1)^m \lambda_{y2}\theta_{jx2l} + (-1)^k \lambda_{x2}\theta_{jy2l} - z_{j3lk} + (-1)^m \lambda_{y2}\theta_{jx3lk}\right\} \\ + c_{23}\left\{\dot{z}_{j2l} - (-1)^m \lambda_{y2}\dot{\theta}_{jx2l} + (-1)^k \lambda_{x2}\dot{\theta}_{jy2l} - \dot{z}_{j3lk} + (-1)^m \lambda_{y2}\dot{\theta}_{jx3lk}\right\} \end{aligned} \tag{16}$$

where, the subscripts relative to the motion of the bogies are described as: k=1, 2 respectively indicate the front and rear axles of the rear bogie, m=1, 2 respectively indicate the left and right sides of the bogie. $v_{jxlkm}(t)$, $v_{jylkm}(t)$ and $v_{jzlkm}(t)$ denote the forces caused by the extension of the lower springs in relative directions, respectively.

y_{j3lk}: Lateral displacement of the wheelset

$$m_3\ddot{y}_{j3lk} + \sum_{m=1}^{2}(-1)^m v_{jylkm}(t) = -\sum_{m=1}^{2} P_{jylkm}(t) \tag{17}$$

z_{j3lk} :Vertical displacement of the wheelset

$$m_3\ddot{z}_{j3lk} - \sum_{m=1}^{2} v_{jzlkm}(t) = -\sum_{m=1}^{2} P_{jzlkm}(t) \tag{18}$$

θ_{jx3lk} :Rolling of the wheelset

$$I_{x3}\ddot{\theta}_{jx3lk} + \sum_{m=1}^{2}(-1)^m \lambda_{y2} v_{jzlkm}(t) = -r\sum_{m=1}^{2} P_{jylkm}(t) + (-1)^m \lambda_{y1}\sum_{m=1}^{2} P_{jzlkm}(t) \tag{19}$$

θ_{jz3lk} :Yawing of the wheelset

$$I_{z3}\ddot{\theta}_{jz3lk} - \sum_{m=1}^{2}(-1)^{k+m} \lambda_{y2} v_{jxlkm}(t) = -(-1)^m \sum_{m=1}^{2} P_{jxlkm}(t) \tag{20}$$

where, $P_{jxlkm}(t)$, $P_{jylkm}(t)$ and $P_{jzlkm}(t)$ respectively represent the dynamic wheel loads acting on the structure in horizontal, vertical and longitudinal directions. The depiction of the reaction forces from the rail treads acting on a wheelset is shown in Fig. 2.

Actually, $P_{jxlkm}(t)$ is the creeping force in longitudinal direction between the wheel and rail tread; $P_{jzlkm}(t)$ is the normal contact force; $P_{jylkm}(t)$ is the combination of the horizontal creeping force between the wheel and rail tread and the lateral force due to the contact of wheel flange and track, respectively. They can be calculated following the wheel-rail contact theory, which leads to a complicated numerical process (Wakui *et al.* 1995).

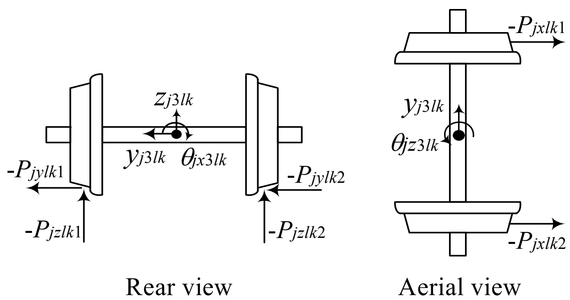

Fig. 2 Contact forces acting on the wheelset

In the present idealization of the train-bridge interaction system, to avoid its complication, instead of calculating the contact forces between the wheel and track structure, the motions of the wheelset are assumed to be compatible with the displacements of the rail structure, while its movement due to the rail irregularities or the wheelset hunting motion is directly inputted. If the yawing motion of the wheelset can be neglected, the motions of the wheelset are represented as follows.

$$y_{j3lk} = \frac{1}{2}\sum_{m=1}^{2} w_{jylkm} \tag{21}$$

$$z_{j3lk} = \frac{1}{2}\sum_{m=1}^{2} w_{jzlkm} \tag{22}$$

$$\theta_{jx3lk} = -(-1)^m \frac{1}{2\lambda_{y1}}\sum_{m=1}^{2} w_{jzlkm} \tag{23}$$

The variables w_{jylkm} and w_{jzlkm} denote the sum of the displacements and irregularities of the rail in y and z-direction, respectively.

$$w_{jylkm} = w_y(t, x_{jlkm}) + z_{0y}(x_{jlkm}) \tag{24}$$

$$w_{jzlkm} = w_z(t, x_{jlkm}) + z_{0z}(x_{jlkm}) \tag{25}$$

where, $w_y(t, x_{jlkm})$ and $w_z(t, x_{jlkm})$ are the displacements of the rail at the contact points of the wheel and the rail in y and z-direction, respectively; and $z_{0y}(x_{jlkm})$ and $z_{0z}(x_{jlkm})$ represent the rail irregularities in y and z-direction, respectively.

$$w_y(t, x_{jlkm}) = \mathbf{\Psi}^{\mathrm{T}}_{jylkm}(t)\mathbf{w}_{\mathrm{b}} \tag{26}$$

$$w_z(t, x_{jlkm}) = \mathbf{\Psi}^{\mathrm{T}}_{jzlkm}(t)\mathbf{w}_{\mathrm{b}} \tag{27}$$

where, $\mathbf{\Psi}_{jylkm}(t)$ and $\mathbf{\Psi}_{jzlkm}(t)$ respectively represent the distribution vectors of y and z-directions that distribute the wheel loads to the ends of the beam elements, and $\mathbf{w}_{\mathrm{b}}$ denotes the nodal displacement vector of the bridge model.

$$\mathbf{\Psi}_{jylkm}(t) = \{0;\cdots;0;\psi_{p,jlkm};\psi_{p+1,jlkm};0;\cdots;0\}^{\mathrm{T}} \tag{28}$$

$$\mathbf{\Psi}_{jzlkm}(t) = \{0;\cdots;0;\psi_{q,jlkm};\psi_{q+1,jlkm};0;\cdots;0\}^{\mathrm{T}} \tag{29}$$

Expanding the equations described above, the differential equations of the train system can be expressed in matrix form as follows.

$$\mathbf{M}_{\mathrm{v}}\ddot{\mathbf{w}}_{\mathrm{v}} + \mathbf{C}_{\mathrm{v}}\dot{\mathbf{w}}_{\mathrm{v}} + \mathbf{K}_{\mathrm{v}}\mathbf{w}_{\mathrm{v}} = \mathbf{f}_{\mathrm{v}} \tag{30}$$

where, $\mathbf{M}_{\mathrm{v}}$, $\mathbf{C}_{\mathrm{v}}$, $\mathbf{K}_{\mathrm{v}}$ and $\mathbf{f}_{\mathrm{v}}$ denote the mass, damping, stiffness matrices and the external force vector of the train system, and $\mathbf{w}_{\mathrm{v}}$ is the displacement vector of vehicle DOFs, respectively.

The wheel loads acting on the bridge, $P_{jylkm}(t)$ and $P_{jzlkm}(t)$, are simplified as follows

$$P_{jylkm}(t) = -\frac{1}{2}m_3\ddot{w}_{jylkm} - (-1)^m v_{jylkm}(t) \tag{31}$$

$$P_{jzlkm}(t) = -\left(\frac{1}{8}m_1 g + \frac{1}{4}m_2 g + \frac{1}{2}m_3 g\right) - \frac{1}{2}m_3\ddot{w}_{jzlkm} + v_{jzlkm}(t) \tag{32}$$

3.2 Formulation of the bridge motion

The differential equation of the bridge is derived as follows, based on FEM and D'Alembert's Principle, which are the typical theory that can be found in various references (Clough and Penzien 1975, Bathe 1982, Weaver and Johnston 1987), thus are not explained in detail here.

$$\mathbf{M}_\mathrm{b}\ddot{\mathbf{w}}_\mathrm{b} + \mathbf{C}_\mathrm{b}\dot{\mathbf{w}}_\mathrm{b} + \mathbf{K}_\mathrm{b}\mathbf{w}_\mathrm{b} = \mathbf{f}_\mathrm{b} \tag{33}$$

where, $\mathbf{M}_\mathrm{b}$, $\mathbf{C}_\mathrm{b}$ and $\mathbf{K}_\mathrm{b}$ denote mass, damping and stiffness matrices of the bridge system, respectively.

Herein, the damping matrix of bridge $\mathbf{C}_\mathrm{b}$ is assumed to be calculated by the linear relation between mass and stiffness matrices, i.e., Rayleigh damping (Agabein 1971), as follows

$$\mathbf{C}_\mathrm{b} = p_1\mathbf{M}_\mathrm{b} + p_2\mathbf{K}_\mathrm{b} \tag{34}$$

where, p_1 and p_2 are the ratio coefficients.

$$p_1 = \frac{2\omega_{\mathrm{b}1}\omega_{\mathrm{b}2}(h_{\mathrm{b}1}\omega_{\mathrm{b}2} - h_{\mathrm{b}2}\omega_{\mathrm{b}1})}{\omega_{\mathrm{b}2}^2 - \omega_{\mathrm{b}1}^2} \tag{35}$$

$$p_2 = \frac{2(h_{\mathrm{b}2}\omega_{\mathrm{b}2} - h_{\mathrm{b}1}\omega_{\mathrm{b}1})}{\omega_{\mathrm{b}2}^2 - \omega_{\mathrm{b}1}^2} \tag{36}$$

where, $\omega_{\mathrm{b}1}$ and $\omega_{\mathrm{b}2}$respectively denote the first and second natural circular frequencies of the bridge model; $h_{\mathrm{b}1}$ and $h_{\mathrm{b}2}$is the damping constants corresponding to $\omega_{\mathrm{b}1}$ and $\omega_{\mathrm{b}2}$, respectively.

Assuming the total number of cars as h, the external force vector $\mathbf{f}_\mathrm{b}$ can be represented as follows

$$\mathbf{f}_\mathrm{b} = \sum_{j=1}^{h}\sum_{l=1}^{2}\sum_{k=1}^{2}\sum_{m=1}^{2}\left\{\mathbf{\Psi}_{jylkm}(t)P_{jylkm}(t) + \mathbf{\Psi}_{jzlkm}(t)P_{jzlkm}(t)\right\} \tag{37}$$

where, $P_{jylkm}(t)$ and$P_{jzlkm}(t)$ are the wheel loads of the train and $\mathbf{\Psi}_{jylkm}(t)$ and $\mathbf{\Psi}_{jzlkm}(t)$ are the distribution vectors.

The vector of nodal displacement of the bridge, $\mathbf{w}_b$, is derived from modal analysis method and represented as follows.

$$\mathbf{w}_b = \sum_{i=1}^{n}\boldsymbol{\varphi}_i q_i = \mathbf{\Phi}\cdot\mathbf{q} \tag{38}$$

where, $\mathbf{q}$ is the generalized coordinate vector of the bridge and $\mathbf{\Phi}$ is the modal matrix composed of the natural modal vector of the bridge $\boldsymbol{\varphi}_i$.

$$\mathbf{q} = \{q_1 \quad q_2 \quad \cdots \quad q_n\}^{\mathrm{T}} \tag{39}$$

$$\mathbf{\Phi} = \{\boldsymbol{\varphi}_1 \quad \boldsymbol{\varphi}_2 \quad \cdots \quad \boldsymbol{\varphi}_n\} = \begin{bmatrix} \phi_{11} & \phi_{12} & \cdots & \phi_{1n} \\ \phi_{21} & \ddots & & \vdots \\ \vdots & & \ddots & \vdots \\ \phi_{m1} & \cdots & \cdots & \phi_{mn} \end{bmatrix} \tag{40}$$

where, the subscript m indicates the number of freedoms of the bridge finite element model after matrix condensation, and n denotes the highest mode number considered.

Substituting $\mathbf{w}_\mathrm{b}$ into Eq. (36), the following equation can be derived

$$\mathbf{M}_\mathrm{b}\mathbf{\Phi}\ddot{\mathbf{q}} + \mathbf{C}_\mathrm{b}\mathbf{\Phi}\dot{\mathbf{q}} + \mathbf{K}_\mathrm{b}\mathbf{\Phi}\mathbf{q} = \mathbf{f}_\mathrm{b} \tag{41}$$

Multiplying both sides by $\mathbf{\Phi}^\mathrm{T}$, the following equation is obtained

$$\mathbf{\Phi}^\mathrm{T}\mathbf{M}_\mathrm{b}\mathbf{\Phi}\ddot{\mathbf{q}} + \mathbf{\Phi}^\mathrm{T}\mathbf{C}_\mathrm{b}\mathbf{\Phi}\dot{\mathbf{q}} + \mathbf{\Phi}^\mathrm{T}\mathbf{K}_\mathrm{b}\mathbf{\Phi}\mathbf{q} = \mathbf{\Phi}^\mathrm{T}\mathbf{f}_\mathrm{b} \tag{42}$$

where

$$\mathbf{\Phi}^\mathrm{T} = \begin{Bmatrix} \boldsymbol{\varphi}_1 \\ \boldsymbol{\varphi}_2 \\ \vdots \\ \boldsymbol{\varphi}_n \end{Bmatrix} = \begin{bmatrix} \phi_{11} & \phi_{21} & \cdots & \phi_{m1} \\ \phi_{12} & \ddots & & \vdots \\ \vdots & & \ddots & \vdots \\ \phi_{1n} & \cdots & \cdots & \phi_{mn} \end{bmatrix} \tag{43}$$

According to the orthogonality of the normal modal vectors, and that $\boldsymbol{C}_\mathrm{b}$ is linearly composed of $\mathbf{M}_\mathrm{b}$ and $\mathbf{K}_\mathrm{b}$,

while$i\neq j$, $\boldsymbol{\varphi}_i^\mathrm{T}\mathbf{M}_\mathrm{b}\boldsymbol{\varphi}_i = 0$, $\boldsymbol{\varphi}_i^\mathrm{T}\mathbf{K}_\mathrm{b}\boldsymbol{\varphi}_i = 0$, $\boldsymbol{\varphi}_i^\mathrm{T}\mathbf{C}_\mathrm{b}\boldsymbol{\varphi}_i = 0$;

while$i=j$, $\boldsymbol{\varphi}_i^\mathrm{T}\mathbf{M}_\mathrm{b}\boldsymbol{\varphi}_i = M_i$, $\boldsymbol{\varphi}_i^\mathrm{T}\mathbf{M}_\mathrm{b}\boldsymbol{\varphi}_i = K_i$, $\boldsymbol{\varphi}_i^\mathrm{T}\mathbf{M}_\mathrm{b}\boldsymbol{\varphi}_i = C_i$.

Assuming $\mathbf{\Phi}^\mathrm{T}\mathbf{f}_\mathrm{b} - \mathbf{\Phi}^\mathrm{T}\mathbf{M}_\mathrm{b}\ddot{\Delta}_\mathrm{b} = f_i$, the differential equation of the bridge with respect to generalized coordinate can be developed as follows

$$M_i\ddot{q}_i + C_i\dot{q}_i + K_i q_i = f_i \text{ ; fori} = 1, \ldots, n \tag{44}$$

3.3 Coupled equation of train-bridge system in matrix form

Based on the formulation developed above, the coupled equation of train-bridge interaction system can be expressed in matrix form as follows.

$$\begin{bmatrix} \mathbf{M}_\mathrm{b}^* & \mathbf{0} \\ \mathrm{Sym} & \mathbf{M}_\mathrm{v} \end{bmatrix}\begin{Bmatrix} \ddot{\mathrm{q}}_\mathrm{b} \\ \ddot{\mathbf{w}}_\mathrm{v} \end{Bmatrix} + \begin{bmatrix} \mathbf{C}_\mathrm{b}^* & \mathbf{C}_\mathrm{bv} \\ \mathrm{Sym} & \mathbf{C}_\mathrm{v} \end{bmatrix}\begin{Bmatrix} \dot{\mathrm{q}}_\mathrm{b} \\ \dot{\mathbf{w}}_\mathrm{v} \end{Bmatrix} + \begin{bmatrix} \mathbf{K}_\mathrm{b}^* & \mathbf{K}_\mathrm{bv} \\ \mathrm{Sym} & \mathbf{K}_\mathrm{v} \end{bmatrix}\begin{Bmatrix} \mathbf{q}_\mathrm{b} \\ \mathbf{w}_\mathrm{v} \end{Bmatrix} = \begin{Bmatrix} \mathbf{F}_\mathrm{b} \\ \mathbf{F}_\mathrm{v} \end{Bmatrix} \tag{45}$$

where, $\mathbf{M}_\mathrm{b}^*$, $\mathbf{C}_\mathrm{b}^*$ and $\mathbf{K}_\mathrm{b}^*$, respectively denote the mass, damping and stiffness components corresponding to the generalized coordinate of the bridge system; $\mathbf{M}_\mathrm{v}$, $\mathbf{C}_\mathrm{v}$ and $\mathbf{K}_\mathrm{v}$, respectively denote the mass, damping and stiffness components corresponding to the DOF of the train system;

$\mathbf{C}_{bv}$ and $\mathbf{K}_{bv}$, respectively denote the coupled damping and stiffness components between the bridge and train systems. The detailed components of the matrix can accordingly be obtained by expanding the above formula, which are used to create the computer program.

3.4 Validation of train-bridge interaction analysis procedure

To confirm the validity of the developed train-bridge interaction analysis procedure, the analytical results using the 3D train model described above and the 3D Shinkansen viaduct FE model are compared with the field measurement results. The actual field measurements were conducted on the Shinkansen line to measure the bridge vibration. Bullet trains composed of 16 cars were running through the viaduct with its actual operational speed of 270 km/h. The bridge vibration was measured at several points of the viaduct during the bullet trains' passage using accelerometers.

The viaducts,on which field tests are conducted, are built with 24 m-length bridge blocks that are separated with each other and connected only by rail structure at adjacent ends. Each block consists of three 6 m-length center spans and two 3 m cantilever parts, so called hanging parts, at each end. Three blocks (72 m) of the bridge are adopted as the numerical model and modeled as 3D beam elements with six-DOF at each node as shown in Fig. 3. The complete information of the numerical models and analytical conditions can be found in the literature (He and Kawatani *et al.* 2011), thus are not given here in detail.

Considering the boundary condition of the bridge, only the dynamic response of the middle block will be examined. In this analysis, the bridge vibration recorded at point-1 through point-3 of the viaduct in Fig. 3, which respectively indicate the point of cantilever part of the slab, the top of the first pier and the top of the third pier of the viaduct with respect to the train running direction, will be examined.

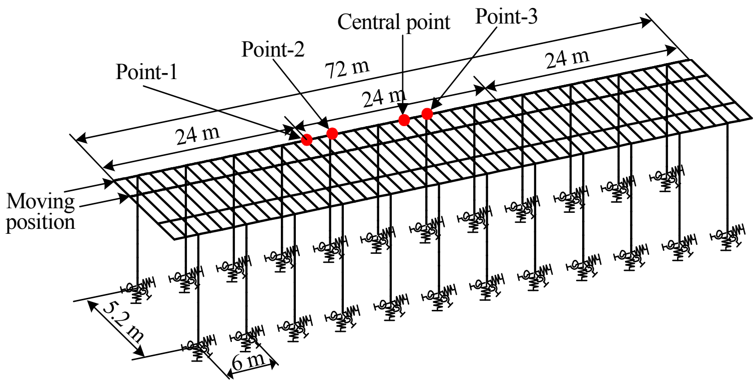

Fig. 3 FEM bridge model

The analytical acceleration responses and the measured ones in vertical and horizontal directions at point-1 through point-3 of the bridge are shown in Figs. 4 and 5, respectively. Here, only the bridge response at Point-3 for the horizontal direction is recorded in the field test. Their maximum (Max) and root-mean-square (RMS) values together with the Fourier spectra are also indicated in the figure. As shown Figs. 4 and 5, the analytical results indicate relatively good agreement with the experimental results, from which the validity of the analytical procedure can be confirmed. Here, the responses at Point-3 display relatively bigger difference between the analysis and experiment, compared with the other points. The reason is considered as follows. Point-3 is far from the hanging part, which induces predominant structural dynamic response because it is a cantilever part. Therefore the vibration amplitude at Point-3 is rather smaller than the other points and significantly influenced by the conditions of rail irregularities and ballast damping effect, which are difficult to be accurately considered in the current model. This can be improved by using more detailed numerical models and providing more accurate analytical parameters and conditions.

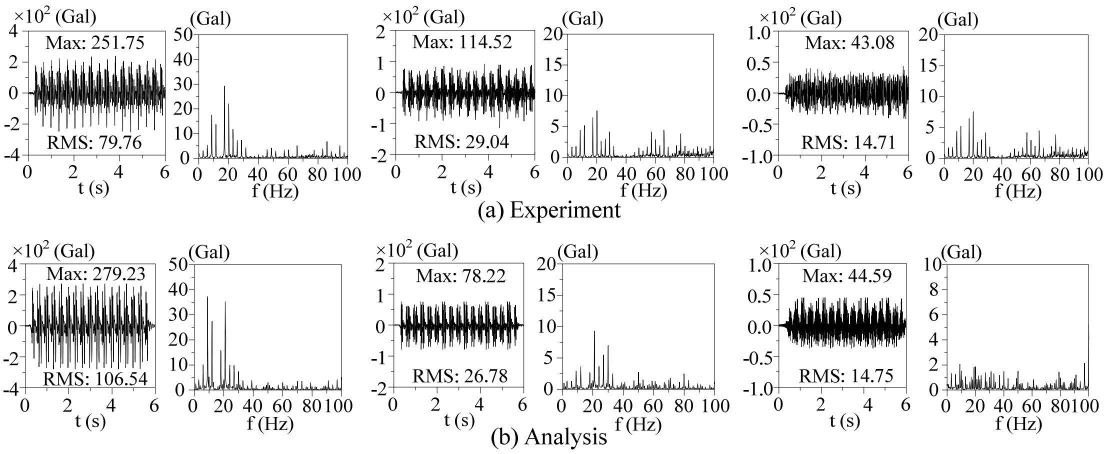

Point-1 Point-2 Point-3

Fig. 4 Bridge acceleration under a moving train (vertical)

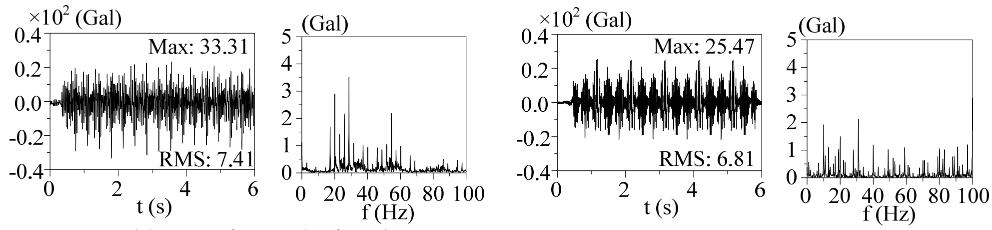

(a) Experiment (Point-3) (b) Analysis (Point-3)

Fig. 5 Bridge acceleration under a moving train (Horizontal)

4. Feasibility investigation of damage detection approach

To investigate the feasibility of the proposed damage detection approach as the preliminary stage of development, a typical simply-supported steel girder bridge in Shinkansen lines of Japan

(Mutsuura 1976), as shown in Fig. 6, is adopted for the numerical evaluation. The properties of the bridge are also indicated in the figure. In general, such a steel girder bridge has a fundamental frequency of about $175/l$ based on the field investigation (Mutsuura 1976), where, l is the length of the girder. In this analysis, as shown in Fig. 6, the girder is modeled with 3D beam elements with six-DOF at each node and uniformly dived into 10 beam elements. The train is assumed to run on an imaginary track rigidly mounted on the girder. Theoretically, the bridge can vibrate three-dimensionally including lateral direction under 3D trains. However, since no excitations exist in other directions, only vertical vibration will occur in the current analyses. The properties of the bridge model are also shown in the figure.

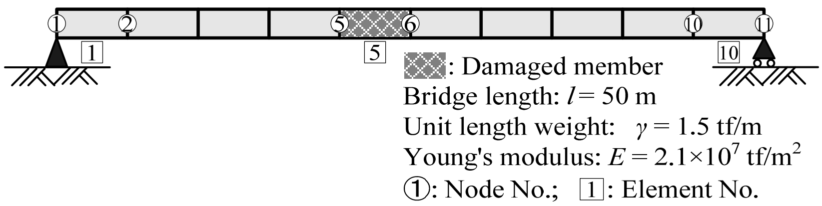

Fig. 6 Simple girder bridge model

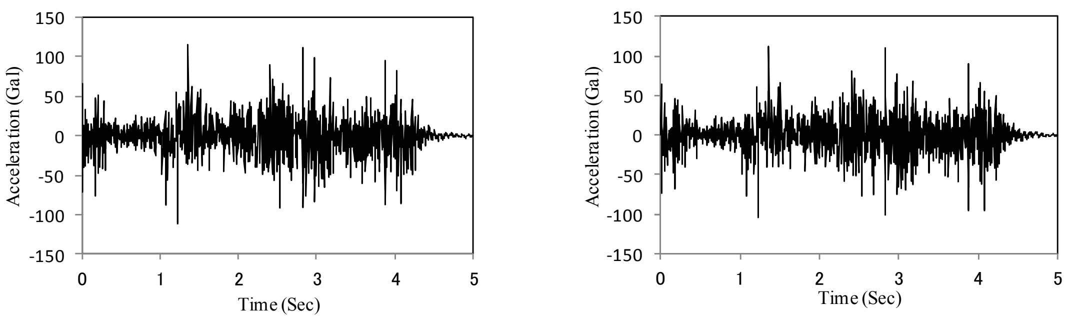

(a) before damage

(b) 30% damage of element 5

Fig. 7 Acceleration responses of the bridge at node No.6

4.1 Possibility investigation of damage detection using bridge dynamic response

To investigate the possibility of using the dynamic response to identify the structural damage, one car of the 3D train model formulized above is used for the analysis. The velocity of the train is assumed as 60 km/h. Then, the following damage condition of the bridge is used. The element No.5 is assumed to have a 30 percent damage due to corrosion, expressed by a 30 percent decrease of its bending moment of inertia.

The eigenvalue analysis of the bridge is performed at first. The first natural frequency before the damage is 3.50 Hz, while after the damage it decreases to 3.37 Hz, and through this, change of the dynamic characteristic can be confirmed. Then, using the developed program for train-bridge interaction based on the above formulization, the acceleration responses at node No.6 before and after the damage are calculated and shown in Fig. 7. The maximum acceleration responses of each node are shown in Table 4. Obvious changing of the acceleration response due to the damage can be confirmed. Therefore, the dynamic responses of the bridge are possible to be used as a criterion to identify the damage. In this paper, since the bridge model is simple, only the acceleration response is used to perform the damage identification. Not to mention, for complicated structures other dynamic response or characteristics, such as displacements, frequencies and mode shapes, etc, may have to be used as the criteria in addition to the accelerations.

Table 4 Acceleration variation due to damage

Node No.	1	2	3	4	5	6	7	8	9	10	11
Max acc (Gal) before damage	30	101	66	114	115	81	141	151	93	253	46
Max acc (Gal) after damage	29	114	67	115	112	79	116	161	161	257	46

4.2 GA Optimization approach

In this paper, the simple GA (Goldberg1989, Koh and Perry 2009) is used for the detection process due to the simplicity of the structure. The flow-chart of GA is shown in Fig. 8. The calibrated crossover rate is set as 60 percent, the mutation rate as 10 percent, and the number of initial population as 50, as recommended in the reference (Koh and Perry 2009). For the bridge structure, the damage degrees of members are treated as discrete values, and each value is encoded by a three binary digits gene string. The definition of the gene strings and the discrete values of damage degrees is given in Table 5, which can detect 0 to 70 percent damage of the structure with an interval of 10 percent. Then, an individual (chromosome) is composed of 10 gene strings corresponding to the 10 finite elements, which is used as the input data for the train-bridge interaction analysis program.

In this analysis, the objective function (OBJ) is defined as the difference between the analytical acceleration response and the measurement data, as Eq. (46). Where, $f(i)$ are the discrete values of the measurement data and $f^*(i)$ are the analytical results, respectively. Here, i and t respectively indicate the number and the total number of the time steps employed in the interaction analyses. In this paper, the simulated dynamic responses of these damage scenarios are assumed as pseudo-measurement data. Here, only the acceleration response of one node (Node 6) is used considering the simple structure. This means only one sensor is needed on the bridge to record the response. Of course, as mentioned above, for actual complex problems dynamic responses of multiple nodes as well as additional dynamic characteristics may be necessary.

$$OBJ = \frac{1}{t}\sum_{i=1}^{t}\{f(i) - f^*(i)\}^2 \tag{46}$$

The effectiveness of the GA algorithm depends greatly on the methods of crossover and mutation as well as the convergence condition, and calibration is needed for a certain problem. In this paper, two-point crossover is adopted, while the mutation is generated by random numbers. The criterion of convergence condition is determined as 10^{-6}.

Table 5 Definition of gene strings

Gene string	000	001	010	011	100	101	110	111
Damage degree (%)	0	10	20	30	40	50	60	70

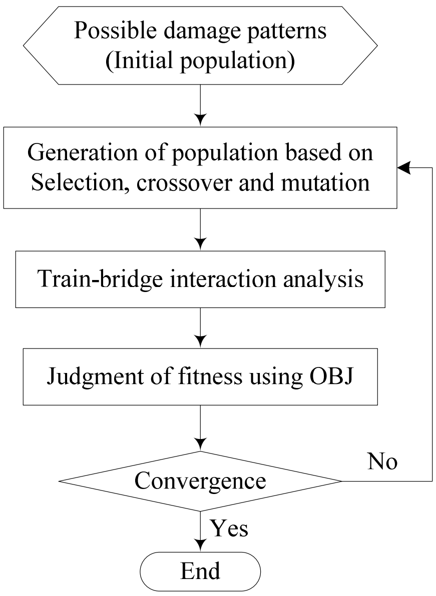

Fig. 8 Flow-chart of GA algorithm

4.3 Damage identification using simple train model

If the dynamic response of the Shinkansen viaducts under daily operating bullet trains can be used for damage detection, it will be remarkably convenient and economical since additional devices and cost can be saved. However, the bridge response due to daily operating trains may be very complicated because of not only the sophisticated dynamic structure of the bullet train itself but also the complex running conditions including the operational velocities as well as the passengers' occupancies in each car, which is expected to bring difficulties for usage as damage identification criterion. The most practical way to carry out the damage detection of the viaducts is to design an inspection train car with as simple as possible dynamic characteristics, which can reduce the dynamic influence of the train on the bridge response to a maximal degree and make the identification process easy. Therefore in this research, a simple two-DOF train car model is used for the damage detection investigation at first, shown in Fig. 9.

Thetwo-DOF train car model is shown in Fig. 9, where variables z_j and θ_j respectively indicate the DOFs of the bouncing and pitching of the car body. This is a simplified structure of the 3D train model described previously and its formulation process can be easily derived from that of the 3D model, thus will not be described in detail here. The detailed information and formulation process of the two-DOF train model can also be found in the reference (He and Noda *et al*. 2011).

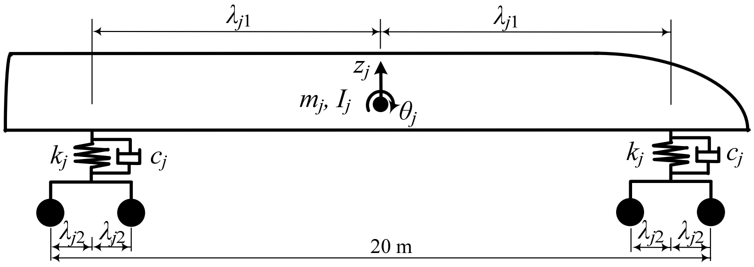

Fig. 9 Two-DOF bullet train car model

4.3.1 Identification for different degrees, locations and numbers of damaged members

To investigate the identification feasibility of the proposed approach under the conditions of different degrees, locations and numbers of damaged members, the following damage scenarios are assumed, which are the targets of identification. The velocity of the train is set as 60 km/h for all the cases.

- Case-1: the element No.5 is assumed to have 11 percent damage.
- Case-2: the element No.5 has 41 percent damage.
- Case-3: the element No.1 has 11 percent damage.
- Case-4: 21 percent damage in element No.1 and a 41 percent damage in element No.5.

Here, the damage of a member is expressed by a uniform decrease of the bending stiffness. For example, if an element has 11 percent damage, then the element loses 11 percent of bending stiffness. The damage location is naturally the location of the damaged member, which means that smaller size of the element will lead to more accurate detection of the damage location. A damage pattern is then defined as the combination of damage degrees and locations.

In this paper, instead of real measurement, the simulated dynamic responses of these assumed scenarios are used as pseudo-measurement data. The calculated bridge responses due to defined possible/detectable damage patterns are then compared with the pseudo-measurement data to find the solution. In the current investigation, the possible/detectable damage degrees in the GA program are assumed to be seven values, which are respectively 10, 20, 30, 40, 50, 60 and 70 percent. In a real bridge, possible damage degrees are almost innumerable. Even if it is not possible to code all of them in the program, enough number of damage degrees at sufficiently small intervals should be defined, because the actual damage degree is not known in advance. The interval should be determined to ensure the identification results to have an acceptable engineering accuracy. On the contrary, if the actual damage degree is known in advance, the possible degrees can be limited to a small number. That is why only seven possible damage degrees are defined in this paper.

In actual recorded vibration data, there will be signal noise included, which brings differences between the analytical results and the recorded ones. In the current investigation, the signal noise is not directly added to the pseudo-measurement data due to its complexity. Instead, the damage degrees used to calculate the pseudo-measurement response are set as 11, 21 and 41 percent, which are slightly different with those of detectable damage one that are 10, 20 and 40 percent. This will virtually provide a noise effect of the data. Of course, more realistic discussion such as applying white noise into the pseudo-measurement data should be made in further investigations.

In structural identification problem, it is desirable to use a small number of sensors as possible due to not only the costs but also the limit of sensor locations. Thus in this analysis, only the Node No.6 is used as the observed point. Then, Case-1 expresses the situation in which the sensor location is near to the damaged member and the damage is moderate, while Case-2 indicates a severe damage state. Case-3 indicates that the sensor is far from moderate damage, and Case-4 represents a situation of multiple damage members.

The identification results using the two-DOF train model based on the approach described so far are shown in Table 6 for all cases assumed. The values of damage degrees for all elements are indicated for both pseudo-measurement data and analytical results. For all cases, the input damage patterns having the nearest damage degrees to the measurements give the best fitness, thus can be identified. The convergence generation for each case is also given in the table. The calculation time of one generation for each case is almost the same, thus the identification efficiency can be evaluated using the convergence generation. From the convergence generation, bigger damage degree cases need longer calculation time and the multiple damage location case needs the longest time to be identified.

Table 6 Identification results for different damage cases

Elem. No.	Case-1		Case-2		Case-3		Case-4	
	Measured	Analysis	Measured	Analysis	Measured	Analysis	Measured	Analysis
1	0	0	0	0	11	10	21	20
2	0	0	0	0	0	0	0	0
3	0	0	0	0	0	0	0	0
4	0	0	0	0	0	0	0	0
5	11	10	41	40	0	0	41	40
6	0	0	0	0	0	0	0	0
7	0	0	0	0	0	0	0	0
8	0	0	0	0	0	0	0	0
9	0	0	0	0	0	0	0	0
10	0	0	0	0	0	0	0	0
Converged generation	12		40		12		265	

4.3.2 Identification for different numbers and speeds of running trains

To discuss the influences of different numbers and speeds of the running trains, the following scenarios are designed. 11 percent damage of the element No.5 is assumed and the two-DOF train model is used for all cases.

- Case-5:one car is running on the bridge with the speed of 120 km/h.
- Case-6: one car is running on the bridge with the speed of 270 km/h.

- Case-7: 16 cars are running under the speed of 120 km/h.
- Case-8: 16 cars are running under the speed of 270 km/h.

The identification results of the above scenarios are then shown in Table 7. The values of damage degrees for all members are also indicated for both pseudo-measurement data and analytical results. For all cases, the input damage patterns having the nearest damage degrees to the pseudo-measurements are identified properly. For one running car cases, the convergence generations are on a similar level, while for 16 running cars cases, the convergence generations increased under high speeds.

For the discussion of convergence generation so far, the tendency is that the case with complicated dynamic response needs longer calculation time. The reason can be considered as that in the current objective function, only the acceleration time history, which is sensitive to the dynamic load and damage conditions, is used as the judgment criterion. This will greatly influence the evolution process of GA. Therefore, in the future work and in real world applications, various dynamic characteristics of the bridge should be used in the objective function to avoid expected deficiencies such like localized solutions.

Table 7 Identification results for different running conditions

Elem. No.	Case-5		Case-6		Case-7		Case-8	
	Measured	Analysis	Measured	Analysis	Measured	Analysis	Measured	Analysis
1	0	0	0	0	0	0	0	0
2	0	0	0	0	0	0	0	0
3	0	0	0	0	0	0	0	0
4	0	0	0	0	0	0	0	0
5	11	10	11	10	11	10	11	10
6	0	0	0	0	0	0	0	0
7	0	0	0	0	0	0	0	0
8	0	0	0	0	0	0	0	0
9	0	0	0	0	0	0	0	0
10	0	0	0	0	0	0	0	0
Converged generation	8		9		153		169	

4.4 Damage Identification using 3D train model

Though the identification process using actual operating bullet train-induced vibration data is expected to be difficult, it is still attractive considering its convenience. If the abnormality of the structure can be detectable even without high accuracy of the damage degrees and locations, it will still be beneficial and can be used as an initial screening method. Therefore, the damage identification using the 3D train model is investigated in this part.

The train is assumed to be composed of 16 cars just as its actual operational condition. The damage scenarios are the same as those of the two-DOF train model. For Case-1 to Case-4, the train velocity is also set as 60 km/h and the identification results are given in Table 8. As shown in Table 8, under the low running speed the damages are also detectable using the 3D train model, though the convergence generations greatly increased compared with those of the two-DOF model.

However, for Case-5 to Case-8 with high running speeds, the damages become undetectable by using the 3D train model. The calculations could not converge within the upper limit of generation, which is set as 1000. The reason is considered as that the bridge response under real train model with high speed becomes highly complicated, and the simple GA searching process may fall into localized solution, which indicates the necessity of an improvement of the GA algorithm. Also, the problem may also be solved by using observation responses of multiple nodes and additional dynamic characteristics of the bridge as the components of the objective function in further investigations.

Table 8 Identification results by 3D train model

Elem. No.	Case-1		Case-2		Case-3		Case-4	
	Measured	Analysis	Measured	Analysis	Measured	Analysis	Measured	Analysis
1	0	0	0	0	11	10	21	20
2	0	0	0	0	0	0	0	0
3	0	0	0	0	0	0	0	0
4	0	0	0	0	0	0	0	0
5	11	10	41	40	0	0	41	40
6	0	0	0	0	0	0	0	0
7	0	0	0	0	0	0	0	0
8	0	0	0	0	0	0	0	0
9	0	0	0	0	0	0	0	0
10	0	0	0	0	0	0	0	0
Converged generation	57		43		187		381	

5. Conclusions

In this research, a damage detection approach is proposed and preliminarily established, using the train-induced vibration response of the bridge. In this approach, only direct structural analysis is employed via the introduction of soft computing methods. The developed train-bridge interaction analysis program is validated by comparing the numerical results with the field test data. The basic concept and process of the proposed damage detection approach is presented in this paper, and its feasibility is numerically investigated using different train models and a simple girder bridge model. A two-DOF train model, which is intended as a designed simple inspection car, is proposed. It is numerically confirmed that the bridge damages under various scenarios are possible to be efficiently identified using the two-DOF model. Therefore, the proposed approach is considered feasible for future actual application. On the other hand, in the case of using realistic 3D train model, only damage cases under low running speeds are detectable. When the train speed is high, it becomes difficult to identify the damages, which indicates the necessity to improve the detection approach.

Further improvements on the current established identification approach, by using sophisticated bridge structure and upgraded GA algorithms, are necessary for real applications. More realistic complex analytical conditions, including measurement noise, should be applied in the future analyses. Also, the numerical procedure needs eventually to be validated by experiments or field test results.

References

Agabein, M.E. (1971), “The effect of various damping assumptions on the dynamic response of structure”, *Bull. Int. Inst. Seismology Earthq. Eng.*, **8**, 217-236.

Alvandi, A. and Cremona, C. (2006), “Assessment of vibration-based damage identification techniques”, *J. Sound Vib.*, **292**, 179-202.

Bathe, K.J. (1982), *Finite element procedures in engineering analysis*, Prentice-Hall, Englewood Cliffs, N. J.

Clough R.W. and Penzien J. (1975), *Dynamics of structures*, McGraw-Hill, Inc.

Doebling, S.W., Farrar, C.R. and Prime, M.B. (1998), “A summary review of vibration-based damage identification methods”, *Shock Vib. Digest*, **30**(2), 91-105.

Goldberg, D.E. (1989), *Genetic algorithms in search, optimization, and machine learning*, Addison Wesley longman, Inc.

He, X., Kawatani, M., Hayashikawa, T. and Matsumoto, T. (2011), “Numerical analysis on seismic response of Shinkansen bridge-train interaction system under moderate earthquakes”, *Earthq. Eng. Eng. Vib.*, **10**(1), 85-97.

He, X., Noda, Y., Hayashikawa, T., Kawatani, M. and Matsumoto, T. (2011), “An analytical approach to coupled vibration of curved rationalized girder bridges and running vehicles”, *Proceedings of the 12th East Asia-Pacific Conference on Structural Engineering and Construction (EASEC-12)*, Procedia Engineering (Elsevier Ltd.).

Kartam, N., Flood, I., Garrett, J.H. and Agrawal, G. (1997), *Artificial neural networks for civil engineers: fundamentals and applications*, American Society of Civil Engineers.

Kawatani, M., KIM, C.W., Doi, H. and Toshinami, T. (2012), “Damage identification of bridges using traffic-induced vibration data”, *Proceedings of the 2012 World Congress on Advances in Civil, Environmental, and Materials Research (ACEM’12)*, 2103-2113, CD-ROM.

Kim, C.W., Kawatani, M. and Kim, K.B. (2005), “Three-dimensional dynamic analysis for Bridge-vehicle Interaction with Roadway roughness”, *Comput. Struct.*, **83**, 1627-1645.

Kim, C.W. and Kawatani, M. (2008), “Pseudo-static approach for damage identification of bridges based on coupling vibration with a moving vehicle”, *Struct. Infrastruct. E.*, **4**(5), 371-379.

Kim, C.W., Isemoto, R., Sugiura, K. and Kawatani, M. (2012), “Structural diagnosis of bridges using traffic-induced vibration measurements”, *Proceedings of the 6th International Conference on Bridge Maintenance, Safety and Management (IABMAS 2012)*, 1-8, CD-ROM.

Kim, C.W., Kawatani, M. and Hao, J. (2012), “Modal parameter identification of short span bridges under a moving vehicle by means of multivariate AR model", *Struct. Infrastruct. E.*, **8**(5), 459-472.

Koh, C.G. and Perry, M.J. (2009), *Structural identification and damage detection using genetic algorithms*, CrcPr I Llc.

Matsuura, A. (1976), "A study of dynamic behavior of bridge girder for high speed railway", *Proceedings of the Japan Society of Civil Engineers*, **256**, 35-47, (In Japanese).

Newmark, N.M. (1959), "A method of computation for structural dynamics", *J. Eng. Mech. - ASCE*, **85**(3), 67-94.

Ni, Y.Q., Zhou, H.F., Chan, K.C. and Ko, J.M. (2008), "Modal flexibility analysis of cable-stayed bridge Ting Kau bridge for damage identification", *Comput. Aided Civil. Infrastruct. E.*, **23** (3), 223-236.

Perry, M.J., Koh, C.G. and Choo, Y.S. (2006), "Modified genetic algorithm strategy for structural identification", *Comput. Struct.*, **84**, 529-540.

Siringoringo, D.M. and Fujino, Y. (2006), "Observed dynamic performance of the Yokohama Bay Bridge from system identification using seismic records", *Struct. Control Health Monit.*, **13**, 226-244.

Wakui, H., Matsumoto, N., Matsuura, A. and Tanabe M. (1995), "Dynamic interaction analysis for railway vehicles and structures", *J. Struct. Earthq. Eng. - JSCE*, **31**(513), 129-138, (in Japanese).

Weaver, W. Jr. and Johnston, P.R. (1987), *Structural dynamics by finite elements*, Prentice-Hall, Inc.

Yoshida, I., Kim, C.W. and Kawatani, M. (2006), "Simulation of damage identification for bridges based on coupling vibration with moving vehicles", *Proceedings of the 4th International Symposium on Steel Structures (ISSS '06)*.

Yoshida, I., Kim, C.W. and Kawatani, M. (2008), "Regularization of inverse problem for damage detection", *Proceedings of the 4th International Conference on Bridge Maintenance, Safety and Management (IABMAS2008)*.

Yun, C.B. and Bahng, E.Y. (2000), "Substructural identification using neural networks", *Comput. Struct.*, **77**, 41-52.

Zhan, J.W., Xia, H., Chen, S.Y. and De Roeck, G. (2011), "Structural damage identification for railway bridges based on train-induced bridge responses and sensitivity analysis", *J. Sound Vib.*, **330**, 757-770.